

HADRONIC PRODUCTION OF J/ψ AND Υ : TRANSVERSE MOMENTUM DISTRIBUTIONS

R. BAIER and R. RÜCKL¹

Fakultät für Physik, Universität Bielefeld, D-4800 Bielefeld 1, Fed. Rep. Germany

Received 16 March 1981

In the framework of perturbative QCD, we calculate inclusive p_T spectra and integrated cross sections for the J/ψ and Υ resonances produced in high-energy proton–proton collisions. We consider the hard scattering processes $gg \rightarrow {}^3S_1 g$ and $gq \rightarrow {}^3P_{0,1,2} q$ with subsequent decay ${}^3P_J \rightarrow {}^3S_1 \gamma$ as the main mechanisms at large transverse momenta. The production at low p_T is described by the subprocesses $gg \rightarrow {}^3P_{0,2} \rightarrow {}^3S_1 \gamma$. The coupling of the heavy S- and P-wave bound states to gluons is treated in the nonrelativistic approximation familiar from the quarkonium model. We present a detailed comparison of this model with the measurements of various experiments. Within the uncertainties inherent in the model it is consistent with the data.

An extensive amount of data on the hadronic production of high-mass electron and muon pairs is now available. Above a smooth continuum one observes heavy resonances. The most prominent of them are the J/ψ and the Υ . The measured cross sections imply that the resonances are produced strongly, whereas the continuum originates from an electromagnetic process. The latter is identified to be the well-known Drell–Yan mechanism. For the resonance production, on the other hand, a sizeable number of processes and models have been proposed. There is along list of publications [1]. For brevity, we only mention the class of models which gained the widest consideration.

These models [2] are based on the assumption that heavy resonances are produced via the QCD subprocesses $q\bar{q} \rightarrow Q\bar{Q}$ and $gg \rightarrow Q\bar{Q}$. Large transverse momenta are considered as originating from the higher-order processes $gg \rightarrow Q\bar{Q}g$, $gq \rightarrow Q\bar{Q}q$ and $q\bar{q} \rightarrow Q\bar{Q}g$ [3]. Semi-local duality [4] arguments are then used to project out from the unbound quark–antiquark production the contribution to $Q\bar{Q}$ bound states. By this procedure one does not consider explicitly the spin and color singlet properties of the resonances. Absolute

normalizations depend on the duality factor which is essentially a free parameter.

In this letter we examine an approach [5] in which, contrary to the duality models, the coupling of the heavy quark bound states is evaluated explicitly. This is done in a nonrelativistic approximation which neglects the relative momentum of the $Q\bar{Q}$ pair with respect to the quark mass m_Q . Focussing on proton–proton collisions at high energies we are considering the following subprocesses:

$$(A) \quad gg \rightarrow {}^3P_{0,2} \rightarrow {}^3S_1 \gamma, \quad (1)$$

$$(B) \quad gg \rightarrow {}^3S_1 g, \quad (2a)$$

$$gq \rightarrow {}^3P_{0,1,2} q \rightarrow {}^3S_1 \gamma q. \quad (2b)$$

A typical set of diagrams is displayed in figs. 1 and 2 which also define our notation. It is understood to add all possible permutations of the gluon lines. The effective coupling of the S-wave in process (2a) is proportional to its radial wavefunction at the origin, $R_S(0)$, whereas the P-waves in (1) and (2b) couple proportional to the derivative of their wavefunctions, $R'_P(0)$. The particular spin and color singlet nature of the bound states is taken care of by appropriate spin and color projection operators. The rest of the loops is calculated in lowest order QCD. The P-waves produced in the

¹ On leave of absence from the Sektion Physik, Universität München, D-8000 München 2, Fed. Rep. Germany.

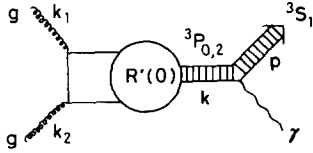


Fig. 1. Diagram which contributes to the subprocesses $gg \rightarrow {}^3P_{0,2} \rightarrow {}^3S_1 \gamma$. Momentum labels are indicated.

processes (1) and (2b), finally, contribute to the observed 3S_1 rates via the radiative decays ${}^3P_J \rightarrow {}^3S_1 \gamma$.

It is easy to see that the processes listed above can also be distinguished as follows. The formation processes of class (A), which have already been considered earlier [6] lead only to 3S_1 states with small transverse momenta since the mass difference between P- and S-waves is typically 400 MeV. We reconsider these processes here to obtain a complete and consistent description of the 3S_1 production for all p_T . The hard scattering processes of class (B), although of higher order in α_S , dominate high p_T production. The contribution of the direct process (2a) to the J/ψ production was discussed in ref. [7]. We evaluate in addition the cascade processes (2b), which are expected to be important in the large p_T domain since the quark distributions are significantly harder than the gluon distribution and the branching ratios $B({}^3P_J \rightarrow {}^3S_1 \gamma)$ are as big as 30% for

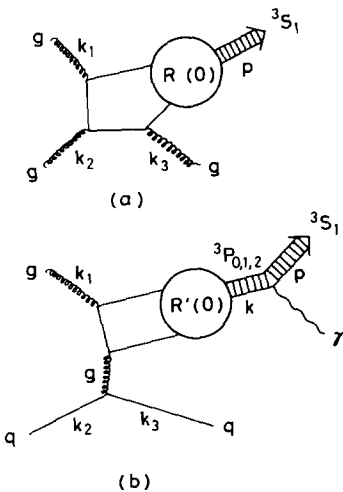


Fig. 2. Diagrams which contribute to the subprocesses (a) $gg \rightarrow {}^3S_1 g$ and (b) $gq \rightarrow {}^3P_{0,1,2} q \rightarrow {}^3S_1 \gamma q$. Momentum labels are indicated.

$J = 1$. For the former reason we also expect $gq \rightarrow {}^3P_J q$ to dominate over $gg \rightarrow {}^3P_J g$.

In the following, we calculate the p_T -distributions $B_{ee} E d^3\sigma/dp^3|_{y=0}$ and the integrated rates $B_{ee} \times d\sigma/dy|_{y=0}$ for both the J/ψ and the Υ resonances. We compare our results in detail with available data at FNAL and ISR energies.

The cross sections for the subprocesses, eqs. (1) and (2), follow from a somewhat lengthy, otherwise straightforward calculation of the diagrams shown in fig. 1 and 2. Details can be found in the existing literature. In particular, the amplitude for $qq \rightarrow {}^3S_1 g$ is obtained from the amplitude for the 3g-decay ${}^3S_1 \rightarrow 3g$ [8] by crossing. The cross sections for the P-wave production via the processes (1) and (2b) are derived [9] from amplitudes given in ref. [10]. Parametrizing the wavefunction $R_S(0)$ by the leptonic width

$$\Gamma_{ee} \equiv \Gamma({}^3S_1 \rightarrow e^+e^-) = 4\alpha^2 e_Q^2 M^{-2} R_S^2(0), \quad (3)$$

and $R'_P(0)$ by the dimensionless ratio

$$r = 4R'_P(0)/M_P^2 R^2(0), \quad (4)$$

we obtain for the processes of class (A):

$$\hat{\sigma}(gg \rightarrow {}^3P_0) = (3\pi^2 \alpha_S^2 r \Gamma_{ee} / 4\alpha^2 e_Q^2 M_0) \delta(\hat{s} - M_0^2), \quad (5a)$$

$$\hat{\sigma}(gg \rightarrow {}^3P_2) = (\pi^2 \alpha_S^2 r \Gamma_{ee} / \alpha^2 e_Q^2 M_2) \delta(\hat{s} - M_2^2), \quad (5b)$$

and for the processes of class (B)

$$\frac{d\hat{\sigma}}{d\hat{t}}(gg \rightarrow {}^3S_1 g) = \frac{5\pi\alpha_S^3 M^2 \Gamma_{ee}}{36\alpha^2 e_Q^2} \times \frac{\hat{s}^2(\hat{s} - M^2)^2 + \hat{t}^2(\hat{t} - M^2)^2 + \hat{u}^2(\hat{u} - M^2)^2}{\hat{s}^2(\hat{s} - M^2)^2(\hat{t} - M^2)^2(\hat{u} - M^2)^2}, \quad (6)$$

$$\frac{d\hat{\sigma}}{d\hat{t}}(qg \rightarrow {}^3P_0 q) = \frac{\pi\alpha_S^3 r \Gamma_{ee} M_0}{18\alpha^2 e_Q^2} \frac{(\hat{t} - 3M_0^2)^2(\hat{s}^2 + \hat{u}^2)}{\hat{s}^2(-\hat{t})(\hat{t} - M_0^2)^4}, \quad (7a)$$

$$\frac{d\hat{\sigma}}{d\hat{t}}(gq \rightarrow {}^3P_1 q) = \frac{\pi\alpha_S^3 r \Gamma_{ee} M_1}{3\alpha^2 e_Q^2} \frac{-4M_1^2 \hat{s}\hat{u} - \hat{t}(\hat{s}^2 + \hat{u}^2)}{\hat{s}^2(\hat{t} - M_1^2)^4}, \quad (7b)$$

$$\frac{d\hat{\sigma}}{d\hat{t}}(gq \rightarrow {}^3P_2 q) = \frac{\pi\alpha_S^3 r \Gamma_{ee} M_2}{9\alpha^2 e_Q^2} \times \frac{-2\hat{s}\hat{u}[\hat{t}^2 - 6M_2^2(\hat{t} - M_2^2)] + (\hat{t} - M_2^2)^2(\hat{t}^2 + 6M_2^4)}{\hat{s}^2(-\hat{t})(\hat{t} - M_2^2)^4} \quad (7c)$$

Here, $M_{0,1,2}$ are the masses of the P-wave states

${}^3P_{0,1,2}$, respectively and M is the mass of the 3S_1 state. According to the nonrelativistic approximation used in deriving these cross sections, we set $2m_Q$ equal to the bound-state mass considered. e_Q is the charge of the heavy quark in units of the electron charge. The invariant variables, finally, are defined as $\hat{s} = (k_1 + k_2)^2$, $t = (k_2 - k_3)^2$ and $\hat{u} = (k_1 - k_3)^2$ with the various 4-momenta assigned in figs. 1 and 2.

Several comments should be made: (i) The above equations exhibit the following characteristic hierarchy. The cross sections (5) contribute to the total 3S_1 rates in order $\alpha_S^2 B({}^3P_J \rightarrow {}^3S_1 \gamma)$, the direct process (6) in order α_S^3 , and the cross sections (7) give contributions of order $\alpha_S^3 B({}^3P_J \rightarrow {}^3S_J \gamma)$. The latter are obviously expected to be a small correction. (ii) Despite this fact, the cascade processes (7) are significant at large p_T since

$$d\hat{\sigma}(gq \rightarrow {}^3P_J q) / d\sigma(gg \rightarrow {}^3S_1 g) \sim p_T^2 / M^2$$

for $p_T^2 \gg M^2$. (iii) One notices that the cross sections (7a) and (7b) have an infrared singularity at $p_T = 0$ due to the gluon propagator \hat{t}^{-1} . This infrared part gives rise to scaling violations in processes (1). In order not to double count we introduce a cutoff in p_T at 1 GeV c . (iv) The 3P_1 resonance cannot be produced by processes of class (A) since it does not couple to two massless gluons.

To obtain the corresponding pp cross sections, the constituent cross sections (5) to (7) have now to be folded with the proper gluon and quark structure functions. This leads to well-known hard scattering expressions. Further, we introduce the decay distributions

$$\Gamma_{\text{tot}}^{-1} d\Gamma({}^3P_J \rightarrow {}^3S_1 \gamma) = \frac{M_J^2 B({}^3P_J \rightarrow {}^3S_1 \gamma)}{\pi(M_J^2 - M^2)} \delta(p^2 - M^2) dp^3 / E, \quad (8)$$

which convert the P-wave spectra into the 3S_1 spectra we focus on. The resulting equations are rather lengthy and will, therefore, be given elsewhere [9] together with the kinematics.

Having the invariant spectra $E d^3\sigma / dp^3$ for the 3S_1 states at hand, we can finally consider possible effects of primordial transverse momenta. We mimic these non-perturbative effects by the following convolution:

$$E d^3\sigma / dp^3 = \int d^2q_T f((p_T - q_T)^2) [E d^3\sigma / dq^3], \quad (9)$$

with

$$f(k_T^2) = (4\pi\sigma^2)^{-1} \exp(-k_T^2 / 4\sigma^2). \quad (10)$$

This simple form serves as an illustration.

Before we present our numerical results we would like to list all parameters which enter. As far as the resonance parameters are concerned, we use for the charmonium system,

$$J/\psi : \quad (11)$$

$$M = 3.096 \text{ GeV}, \quad \Gamma_{ee} = 4.8 \text{ keV}, \quad B_{ee} = 0.076$$

$${}^3P_J :$$

$$M_J = 3.414 \text{ GeV}, \quad B({}^3P_J \rightarrow J/\psi \gamma) = 0.027 \text{ for } J = 0, \\ = 3.507 \text{ GeV}, \quad = 0.315 \text{ for } J = 1, \\ = 3.551 \text{ GeV}, \quad = 0.154 \text{ for } J = 2, \quad (12)$$

These are experimentally measured values [11]. For the ratio r defined in eq. (4) we take

$$r = 0.074, \quad (13)$$

as suggested by a detailed analysis of potential models [12]. In case of the bottomonium system, we have for the Υ [11];

$$\Upsilon :$$

$$M = 9.46 \text{ GeV}, \quad \Gamma_{ee} = 1.3 \text{ keV}, \quad B_{ee} = 0.035 \quad (14)$$

The 3P_J states have not been observed yet. Therefore, we have to rely completely on potential model results [12]

$${}^3P_J :$$

$$M_J \sim 9.9 \text{ GeV}, \\ B({}^3P_J \rightarrow \Upsilon \gamma) \sim 0.04 \text{ for } J = 0, \\ \sim 0.29 \text{ for } J = 1, \\ \sim 0.10 \text{ for } J = 2, \quad (15)$$

and

$$r = 0.013. \quad (16)$$

Note that the branching ratios are very similar to the ones in the charmonium system.

Since the subprocesses (1) and (2) are of order α_S^2 and α_S^3 , respectively, it is clear that the absolute normalization will depend rather sensitively on the scale

Λ of the running coupling constant α_S at least for J/ψ production. We choose $\Lambda = 500$ MeV for the following reasons: (i) This value is used in various other hard scattering processes treated in the leading logarithm approximation. (ii) It is also adopted in the calculation of the QCD corrections to the Drell-Yan process which produces the continuum underneath the J/ψ and Υ . (iii) The same value is used in the potential model analysis of ref. [12]. Here, we should point out that in some of the previous works [6,7] on this subject one has chosen effectively $\Lambda \sim 100$ MeV. This leads to $\alpha_S(M_\psi^2) \sim 0.22$ as extracted from the observed hadronic decays of J/ψ . However, we think that the scale Λ appropriate for the decays of quarkonia is not necessarily the same as the one relevant for the production, since the higher-order corrections are in general different. At any rate, this explains partly why we get higher rates of the J/ψ compared to the results obtained in refs. [6,7]. However, the predictions for Υ suffer much less from this uncertainty since $M_\Upsilon^2 \sim 100$ GeV².

For the quark and gluon structure functions we adopt the parametrizations of ref. [13] which include scale breaking consistent with scaling violation in deep inelastic processes. A minor ambiguity is due to the fact that there are several large scales in the problem, for example, \hat{t} , p_T^2 , $p_T^2 + M^2$ or other combinations. We choose the square of the transverse mass $p_T^2 + M^2$. In order to exhibit the size of scale breaking we also calculate the cross sections in the scaling limit using [14]

$$xG(x) = 3(1-x)^5 \tag{17}$$

and

$$xQ(x) = x[u(x) + d(x) + 4s(x)] \\ = (2.773 + 4.094x)\sqrt{x}(1-x)^3 + 1.26(1-x)^7 \tag{18}$$

α_S is evaluated at the mass of the resonance considered. For the width of the primordial transverse momentum distribution given in eq. (10) we take the same value $\sigma = 0.48$ GeV as used in the analysis of the Drell-Yan process [15].

Having described the calculation we now present our results. The invariant J/ψ -distribution $B_{ee} E d^3\sigma/dp^3$ at rapidity $y = 0$ is shown in fig. 3 and compared with data from refs. [16,17] at three ISR energies. In fig. 4

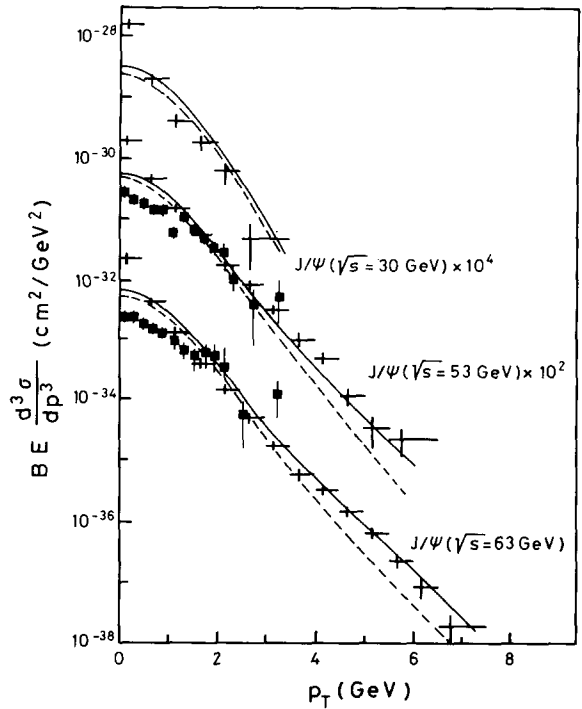


Fig. 3. The invariant cross sections for $pp \rightarrow J/\psi X$ at $y = 0$ as a function of p_T at $\sqrt{s} = 30, 53$ and 63 GeV. The data points are taken from ref. [16] (+) and ref. [17] (■). The solid (dashed) curves show the result of our QCD calculation with scaling (scale breaking) structure functions as described in the text.

we plot the Υ -spectra at $\sqrt{s} = 27.4$ GeV and $\sqrt{s} = 63$ GeV. The data points are taken from refs. [16,18], respectively. Table 1 is a compilation of integrated cross sections $B_{ee} d\sigma/dy|_{y=0}$. The rates calculated in our model are compared with a number of measurements published in refs. [16-20]. Table 1 also gives the percentage of the individual contributions from the various subprocesses (1) and (2). Both, figures and table 1, seem to indicate that the overall agreement of the model with the data is reasonable for J/ψ production and somewhat poorer for Υ production. In the following we discuss in detail a number of aspects which are important for a critical appraisal of the model.

Let us first consider the p_T distributions. In the low p_T region ($p_T < 2$ GeV) the shape of the spectra is entirely determined by the primordial motion. Our results for J/ψ (fig. 3) agree with the experimental distributions of ref. [16] except in the lowest p_T bin

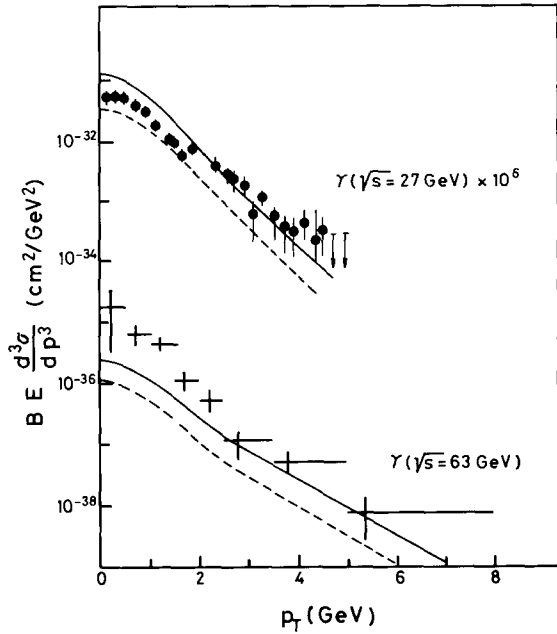


Fig. 4. The invariant cross section for $pp \rightarrow \Upsilon X$ at $y = 0$ as a function of p_T at $\sqrt{s} = 27.4$ and 63 GeV. The data points at $\sqrt{s} = 27.4$ GeV are from ref. [18] (\bullet), the ones at 63 GeV are from ref. [16] (+). The solid (dashed) curves show the result of our QCD calculation with scaling (scale breaking) structure functions as described in the text.

where the prediction comes out too small. However, the same curves are above the data points of ref. [17] for $p_T < 1$ to 1.5 GeV. For Υ production at small transverse momenta (fig. 4), the calculated spectrum is consistent with the data [18] at $\sqrt{s} = 27.4$ GeV, whereas it is considerably lower than the measured distribution [16] at $\sqrt{s} = 63$ GeV. Unfortunately, due to the discrepancies at low p_T in the two data sets [16, 17] displayed in fig. 3, it is not possible to draw a definite conclusion. Trivially, one can narrow or broaden the theoretical curves at low p_T by choosing a smaller or larger value for σ in the parametrization of the non-perturbative primordial p_T distribution of eq. (10). In addition, the normalization at low p_T depends on the parameter r [eq. (5)] which is only determined theoretically within the charmonium model.

For $p_T > 2$ GeV, there is good agreement between the model and the data for both J/ψ and Υ , as far as the slopes are concerned. The absolute normalization comes out quite well for J/ψ and a little low for Υ . Obviously, the slopes do not allow to discriminate between the scaling (full curves) and the scale breaking (dashed curves) structure functions, although absolute normalization favors the somewhat larger rates obtained in the scaling limit. This may indicate that the gluon distribution is still rather hard at $Q^2 > 25$ GeV². The

Table 1
 $Bd\sigma/dy|_{y=0}$ (cm²) for J/ψ and Υ and contributions from different subprocesses (%).

	\sqrt{s} (GeV)	data	ref.	model	process Eq. 1	process Eq. 2a	process Eq. 2b	
J/ψ	30	$(9.1 \pm 2.5) \times 10^{-33}$	[16]	1.2×10^{-32}	55	35	10	(i)
		$(6.58 \pm 1.76) \times 10^{-33}$	[17]	9.5×10^{-33}	56	35	9	(ii)
	53	$(13.6 \times 3.1) \times 10^{-33}$	[16]	2.3×10^{-32}	50	39	11	(i)
		$(1.096 \times 0.041) \times 10^{-32}$	[17]	1.9×10^{-32}	52	36	12	(ii)
	63	$(14.8 \pm 3.3) \times 10^{-33}$	[16]	2.6×10^{-32}	48	38	13	(i)
		$(1.02 \pm 0.07) \times 10^{-32}$	[17]					
		$(1^{+1.0}_{-0.5}) \times 10^{-32}$	[19]	2.2×10^{-32}	51	36	13	(ii)
Υ	27.4	$(4.35 \pm 0.15) \times 10^{-37}$	[18]	5.7×10^{-37}	59	35	6	(i)
				2.0×10^{-37}	59	36	5	(ii)
	63	$(15.2 \pm 5.5) \times 10^{-36}$	[16]	1.4×10^{-35}	53	39	8	(i)
		$(9 \pm 2 \pm 1) \times 10^{-36}$	[20]	6.2×10^{-36}	50	41	9	(ii)

(i) scaling, (ii) scale breaking

primordial motion, discussed above in the context of the low p_T spectra, also affects the high p_T region. At $p_T \sim 4$ to 5 GeV and the highest ISR energies, for example, it enhances the rates for J/ψ by a factor 2 and for Υ by a factor 1.2

A feature which is very characteristic for our model is the relative size of the contributions from the various subprocesses in different kinematical regions (see ref. [9] for details). As already pointed out, the 3S_1 -yields at low p_T are completely dominated by the $^3P_{0,2}$ states produced via $gg \rightarrow ^3P_{0,2}$ and decaying into $^3S_1\gamma$. The 3P_J states, however, contribute also a considerable fraction to the observed J/ψ rates at large p_T . The relevant subprocess, here, is $gq \rightarrow ^3P_Jq$. For illustration, we find a fraction of 20% at $\sqrt{s} = 30$ GeV and $p_T \geq 2$ GeV. This fraction increases with energy and amounts to 30% for $p_T \sim 2$ GeV rising to 60% for $p_T \sim 7$ GeV at the highest ISR energy. On the other hand, only about 10% of the Υ rate is produced via intermediate 3P_J states, rather independently of energy. Consequently, Υ production at large p_T is dominated by the direct process $gg \rightarrow \Upsilon g$. An independent experimental test of this result can be performed by measuring the positive to negative charge ratio of hadrons in the jet opposite to the Υ at large p_T . Since one expects this recoiling jet to be a gluon the ratio should be one. This is in contrast to the duality model of Kunszt et al. [3] which predicts a charge ratio larger than one since the contribution coming from $gq \rightarrow b\bar{b}q$ exceeds the one from $gg \rightarrow b\bar{b}g$. For the jet recoiling against the J/ψ , both models give a charge ratio larger than one. In our model this is due to the contribution from the 3P_J production discussed above.

We now turn to the integrated rates $B_{ee} d\sigma/dy|_{y=0}$ summarized in table 1. One observes that the calculated J/ψ cross sections are, generally, a factor 2 higher than the quoted experimental rates [16,17,19], whereas there is agreement on the Υ rates [16,18,20] within the experimental errors. This is what one expects from a glance at the p_T spectra in figs. 3 and 4 as far as the J/ψ data of ref. [17] and the Υ data of ref. [18] are concerned. However, it is also apparent from these plots, that the integrated rates of ref. [16] should be somewhat larger than the theoretical ones for J/ψ and considerably larger for Υ . This is certainly not what we find in our calculation. A similar discrepancy shows up if one compares the J/ψ data of ref. [16] with the results of another IRS group published in ref. [17].

Although the p_T spectra of the two groups are significantly different for $p_T < 1.5$ GeV, their integrated rates coincide within the errors. There seems to be a normalization problem on the experimental side which complicates the confrontation of our model with the available data. Calculating from the p_T spectra plotted in ref. [16]

$$B_{ee} \left. \frac{d\sigma}{dy} \right|_{y=0} = 2\pi \int \left(B_{ee} E \frac{d^3\sigma}{d^3p} \right)_{y=0} p_T dp_T,$$

we obtain for J/ψ 2 to 3 times and, for Υ 4 times the yields quoted in the same reference. In case of the other data [17,18] shown in fig. 3 and 4 we reproduce the quoted values for $B_{ee} d\sigma/dy|_{y=0}$. The consistency of our model with the p_T distributions of ref. [16], in particular for Υ production, would be improved, if we frankly renormalized their p_T spectra such that they yield the quoted values of $B_{ee} d\sigma/dy|_{y=0}$, on which all experiments [16–20] agree. We should also mention that the Υ rates as defined experimentally contain contributions from Υ' and, partly, even Υ'' which are not included in the theoretical cross sections. Following ref. [18] the Υ' (Υ'') production amounts to 30 (15)% of the measured cross sections.

The model also makes interesting predictions on the relative 3S_1 production rates via the various subprocesses considered. According to table 1 about 2/3 of these rates come from P-wave production and the subsequent decay $^3P_J \rightarrow ^3S_1\gamma$, whereas 1/3 is due to the direct process $gg \rightarrow ^3S_1g$. This large fraction of P-wave states is consistent with the experimental observation [21] that $(47 \pm 8)\%$ of the inclusive J/ψ production proceeds via the $\chi(3.5)$ states. A more detailed analysis is given in ref. [9].

In the case of inelastic photoproduction of heavy resonances color prohibits the production of P-waves via subprocesses corresponding to (1) and (2b) with one initial gluon replaced by the photon. In a recent analysis [22] Berger and Jones showed that the remaining direct process $\gamma g \rightarrow ^3S_1g$ allows for a consistent description of the data.

With the complication in the comparison with existing data in mind we would like to conclude that the model presented in this letter describes correctly: (i) the energy dependence of J/ψ and Υ production, (ii) the relative production rates of J/ψ and Υ at a given energy, and (iii) the slopes of the p_T distributions, at least at large transverse momenta. If one ac-

cepts a value for Λ of about 500 MeV, which is by no means unreasonable for lowest-order QCD calculations, the model also predicts absolute rates consistent with data.

One of us (R.R.) would like to thank C. Kourkouvelis, J.H. Kühn and Z. Kunszt for helpful discussions. We both are grateful to I. Stumer for an informative communication.

References

- [1] For a review, see: E. Reya, Perturbative quantum chromodynamics, preprint DESY 79/88, DO TH 29/20 (1979).
- [2] H. Fritzsch, Phys. Lett. 67B (1977) 217; M. Glück, J.F. Owens and E. Reya, Phys. Rev. D17 (1978) 2324; L.M. Jones and H.W. Wyld, Phys. Rev. D17 (1978) 2332; V. Barger, W.Y. Keung and R.J.N. Phillips, Phys. Lett. 91B (1980) 253.
- [3] Z. Kunszt, E. Pietarinen and E. Reya, Phys. Rev. D21 (1980) 733.
- [4] H. Fritzsch and K.H. Streng, Phys. Lett. 72B (1978) 385.
- [5] R. Rückl, Talk Workshop on Lepton pair production (les Arcs, January 1981).
- [6] C.E. Carlson and R. Suaya, Phys. Rev. D14 (1976) 3115.
- [7] Chang Chao-Hsi, Nucl. Phys. B172 (1980) 425.
- [8] See e.g., K. Koller and T. Walsh, Nucl. Phys. B140 (1978) 449.
- [9] R. Baier and R. Rückl, in preparation.
- [10] J.H. Kühn, J. Kaplan and E.G.O. Safiani, Nucl. Phys. B157 (1979) 125.
- [11] K. Berkelman, Talk XXth Intern. Conf. on High energy physics (Madison, 1980).
- [12] H. Krasemann, Z. Phys. C1 (1979) 189.
- [13] R. Baier, J. Engels and B. Petersson, Z. Phys. C2 (1979) 265; Z. Phys. C6 (1980) 309.
- [14] G. Altarelli, R.K. Ellis and G. Martinelli, Nucl. Phys. B157 (1979) 461.
- [15] R.D. Field, Phys. Scr. 19 (1979) 131.
- [16] C. Kourkouvelis et al., Phys. Lett. 91B (1980) 481.
- [17] A.G. Clark et al., Nucl. Phys. B142 (1978) 29.
- [18] K. Ueno et al., Phys. Rev. Lett. 42 (1979) 486.
- [19] D. Antreasyan et al., Proc. EPS Intern. Conf. on High energy physics, (Geneva) (CERN, 1980) p. 779.
- [20] A.L.S. Angelis et al., Phys. Lett. 87B (1979) 398.
- [21] C. Kourkouvelis et al., Phys. Lett. 81B (1979) 405.
- [22] E.L. Berger and D. Jones, Inelastic photoproduction of J/ψ and Υ by gluons, preprint ANL-HEP-PR-80-72 (1980).